



ARL-TR-8236 • DEC 2017



Vapor Pressure of Antimony Triiodide

by Patrick J Taylor, Ryan Enck, Charles Rong, and
Jay R Maddux

Approved for public release; distribution is unlimited.

NOTICES

Disclaimers

The findings in this report are not to be construed as an official Department of the Army position unless so designated by other authorized documents.

Citation of manufacturer's or trade names does not constitute an official endorsement or approval of the use thereof.

Destroy this report when it is no longer needed. Do not return it to the originator.



Vapor Pressure of Antimony Triiodide

by Patrick J Taylor, Ryan Enck, and Charles Rong
Sensors and Electron Devices Directorate, ARL

Jay R Maddux
General Technical Services, Wall Township, NJ

REPORT DOCUMENTATION PAGE

Form Approved
OMB No. 0704-0188

Public reporting burden for this collection of information is estimated to average 1 hour per response, including the time for reviewing instructions, searching existing data sources, gathering and maintaining the data needed, and completing and reviewing the collection information. Send comments regarding this burden estimate or any other aspect of this collection of information, including suggestions for reducing the burden, to Department of Defense, Washington Headquarters Services, Directorate for Information Operations and Reports (0704-0188), 1215 Jefferson Davis Highway, Suite 1204, Arlington, VA 22202-4302. Respondents should be aware that notwithstanding any other provision of law, no person shall be subject to any penalty for failing to comply with a collection of information if it does not display a currently valid OMB control number.

PLEASE DO NOT RETURN YOUR FORM TO THE ABOVE ADDRESS.

1. REPORT DATE (DD-MM-YYYY) December 2017		2. REPORT TYPE Technical Report		3. DATES COVERED (From - To) October 3, 2016 – September 30, 2017	
4. TITLE AND SUBTITLE Vapor Pressure of Antimony Triiodide				5a. CONTRACT NUMBER	
				5b. GRANT NUMBER	
				5c. PROGRAM ELEMENT NUMBER	
6. AUTHOR(S) Patrick J Taylor, Ryan Enck, Charles Rong, and Jay R Maddux				5d. PROJECT NUMBER	
				5e. TASK NUMBER	
				5f. WORK UNIT NUMBER	
7. PERFORMING ORGANIZATION NAME(S) AND ADDRESS(ES) US Army Research Laboratory ATTN: RDRL-SED-E 2800 Powder Mill Road Adelphi, MD 20783-1138				8. PERFORMING ORGANIZATION REPORT NUMBER ARL-TR-8236	
9. SPONSORING/MONITORING AGENCY NAME(S) AND ADDRESS(ES)				10. SPONSOR/MONITOR'S ACRONYM(S)	
				11. SPONSOR/MONITOR'S REPORT NUMBER(S)	
12. DISTRIBUTION/AVAILABILITY STATEMENT Approved for public release; distribution is unlimited.					
13. SUPPLEMENTARY NOTES					
14. ABSTRACT The equilibrium vapor pressure of antimony triiodide (SbI ₃) has been measured over a temperature range from –20 to 47 °C using a classical Knudsen cell method. An analysis of the slope of that data as a function of temperature yields an enthalpy of sublimation (ΔH_{vapor}) value of $\Delta H_{\text{vapor}} = -128.48$ kJ/mol for SbI ₃ .					
15. SUBJECT TERMS thermoelectric, molecular beam epitaxy, MBE, doping, superlattice, enthalpy of vaporization					
16. SECURITY CLASSIFICATION OF:			17. LIMITATION OF ABSTRACT UU	18. NUMBER OF PAGES 16	19a. NAME OF RESPONSIBLE PERSON Patrick J Taylor
a. REPORT Unclassified	b. ABSTRACT Unclassified	c. THIS PAGE Unclassified			19b. TELEPHONE NUMBER (Include area code) (301) 394-1475

Contents

List of Figures	iv
1. Introduction	1
2. Vapor Pressure	1
3. Experiment	3
4. Discussion and Measurements	5
5. Significance	6
6. MBE Doping Strategy	7
7. Conclusions	7
8. References	8
List of Symbols, Abbreviations, and Acronyms	9
Distribution List	10

List of Figures

Fig. 1	(left) Knudsen cell showing the orifice and (right) the ampoule of high-purity SbI_3	3
Fig. 2	Equilibrium vapor pressure of SbI_3 as a function of inverse temperature	4
Fig. 3	Effective ΔH_{vapor} of SbI_3 as a function of temperature	6

1. Introduction

Antimony triiodide (SbI_3) is one of the most effective n-type dopants for $(\text{Bi,Sb})_2(\text{Te,Se})_3$ thermoelectric materials.^{1,2} Precise control of the concentration of the SbI_3 dopant in $(\text{Bi,Sb})_2(\text{Te,Se})_3$ is the key to obtaining good n-type materials, and consequently, the highest-performance thermoelectric devices. There is an ideal amount of SbI_3 that yields an optimum concentration range of 3 to $5 \times 10^{19}/\text{cm}^3$ of n-type carriers.² All commercial bulk thermoelectric devices have doped n-type materials prepared to achieve this n-type dopant concentration range.

To effect n-type doping in bulk materials, an appropriate amount of SbI_3 is added to $(\text{Bi,Sb})_2(\text{Te,Se})_3$ source materials, which are all co-melted at temperatures greater than 600 °C. In the melt, SbI_3 chemically decomposes and liberates free antimony (Sb) and iodine (I) atoms, which become substitutionally incorporated onto the $(\text{Bi,Sb})_2(\text{Te,Se})_3$ crystal lattice during subsequent solidification and Bridgman crystal growth. Substitutional Sb is isoelectronic on a bismuth (Bi) site and has little consequence on doping. However, substitutional I on a tellurium (Te) site will serve as a singly ionized donor, and in the case of I on a Bi or Sb site, will act as a doubly ionized donor. In either of those cases, substitutional I causes n-type conduction.

The growth of epitaxial single-crystal *thin films* of n-type $(\text{Bi,Sb})_2(\text{Te,Se})_3$ materials presents new doping challenges because it is a nonequilibrium process. $(\text{Bi,Sb})_2(\text{Te,Se})_3$ epitaxial materials have been grown by molecular beam epitaxy (MBE)³ and organometallic vapor phase epitaxy (OMVPE) growth techniques.⁴ However, the use of this preferred SbI_3 dopant in either MBE or OMVPE is not reported. MBE and OMVPE are distinct from the bulk technique because crystal growth proceeds by the vapor phase and at a significantly lower temperature, approximately 300 °C. Because the material never melts, the incorporation of SbI_3 into epitaxial films would necessarily proceed by some alternate vapor phase mechanism. The goal of the present work, therefore, is to understand the vapor pressure behavior of SbI_3 as a stepping-stone toward the overall goal of employing SbI_3 during MBE growth to obtain extrinsically doped n-type $(\text{Bi,Sb})_2(\text{Te,Se})_3$ epitaxial materials.

2. Vapor Pressure

In a classical MBE growth process, each individual source material is heated to some temperature (T) to produce an equilibrium vapor having pressure (P) that can be made to condense on a crystalline substrate and epitaxially grow single crystals of the desired chemistry. The production of an equilibrium vapor pressure above

each condensed material is a phase transformation process where there is a net change in molar-specific volume (ΔV) from the condensed phase to its vapor. The rate of that phase change depends on the enthalpy of vaporization (ΔH_{vapor}) and is governed by thermodynamics. The Clausius-Clapeyron relationship shown in Eq. 1 describes the thermodynamics that governs the phase transformation between phases:

$$\frac{dP}{dT} = \frac{(\Delta H_{\text{vapor}})}{\Delta V} \left[\frac{1}{T} \right]. \quad (1)$$

For a phase transformation from a condensed phase to a vapor phase, one may assume the relative change in molar-specific volume (ΔV) is essentially equal to the specific volume of the vapor (V_{vapor}) because vapor phases usually occupy significantly larger volumes than those occupied by condensed phases ($V_{\text{condensed}}$).

$$\Delta V = (V_{\text{vapor}} - V_{\text{condensed}}) \approx V_{\text{vapor}}. \quad (2)$$

If one assumes the obtained vapor behaves according to the ideal gas law, then $V_{\text{vapor}} = RT/P$, where R is the common gas constant (8.314 J/mol-K), and Eq. 1 may be rewritten as

$$\frac{dP}{dT} = \frac{P(\Delta H_{\text{vapor}})}{RT^2}. \quad (3)$$

Rearranging Eq. 3 and integrating between 2 thermodynamic states, say state “1” and state “2”, as per Eq. 4,

$$\int_{P1}^{P2} \frac{dP}{P} = \frac{(\Delta H_{\text{vapor}})}{R} \int_{T1}^{T2} \frac{dT}{T^2} \quad (4)$$

yields the analytical, closed-form Clausius-Clapeyron equation for equilibrium vapor pressure as a function of T evaluated between states 1 and 2:

$$\ln(P) = \frac{(\Delta H_{\text{vapor}})}{RT} \text{ or } P = \exp \left[\frac{(\Delta H_{\text{vapor}})}{RT} \right] + C. \quad (5)$$

Equation 5 predicts an exponential dependence of equilibrium vapor pressure on inverse-temperature with the slope of $(\Delta H_{\text{vapor}}/R)$. One method of experimentally determining ΔH_{vapor} , therefore, is to measure the equilibrium vapor pressure of any material as a function of inverse-temperature where the slope of the data can be used to directly determine ΔH_{vapor} .

3. Experiment

An ampoule of 99.999% pure SbI_3 was loaded into a Knudsen cell fabricated from pyrolytic boron nitride (p-BN). p-BN is chemically nonreactive and inert over the entire temperature range of concern, so there are no chemical effects other than the phase change of SbI_3 within. Care was taken to minimize exposure of SbI_3 to lab air because it is hygroscopic and loses its brilliant orange color (Fig. 1, right) as it adsorbs water from the lab air.

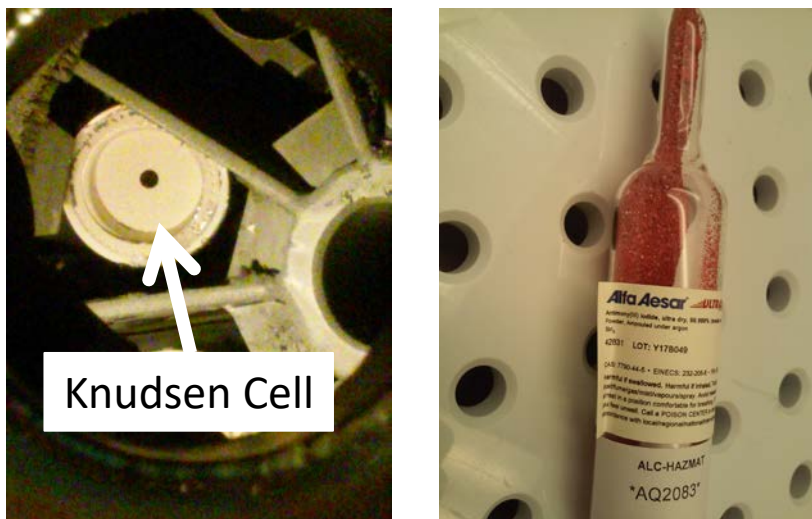


Fig. 1 (left) Knudsen cell showing the orifice and (right) the ampoule of high-purity SbI_3

A Knudsen cell is a special, almost fully enclosed chamber that has a small orifice on one end. A material placed inside the Knudsen cell is heated and will respond by generating an equilibrium vapor pressure inside according to the Clausius-Clapeyron equation. Because some vapor can escape from the small orifice, the equilibrium vapor pressure can be determined by techniques that can quantify the efflux of vapor. Further, the enthalpy of vaporization, ΔH_{vapor} , can be determined by measuring the temperature dependence of that pressure.

The Knudsen cell assembly was mounted onto an MBE system that can achieve vacuum on the order of 10^{-10} Torr. Because of that extremely strong vacuum, vapor pressure measurements can be expanded by more than 10 orders of magnitude compared to previous work. The equilibrium vapor pressure within the MBE is measured by the use of a common hot-cathode Bayard–Alpert gauge.

For the present study, the range of temperatures where the vapor pressure is small was investigated and compared to previously published data from the temperature range where the vapor pressure is relatively high. Three independent measurements of the vapor pressure were conducted in this study and are color-coded red, blue,

and purple in Fig. 2. For each measurement, the temperature of the Knudsen cell was very slowly increased starting from 14 °C and allowing sufficient time for the SbI_3 within the Knudsen cell to reach thermal equilibrium.

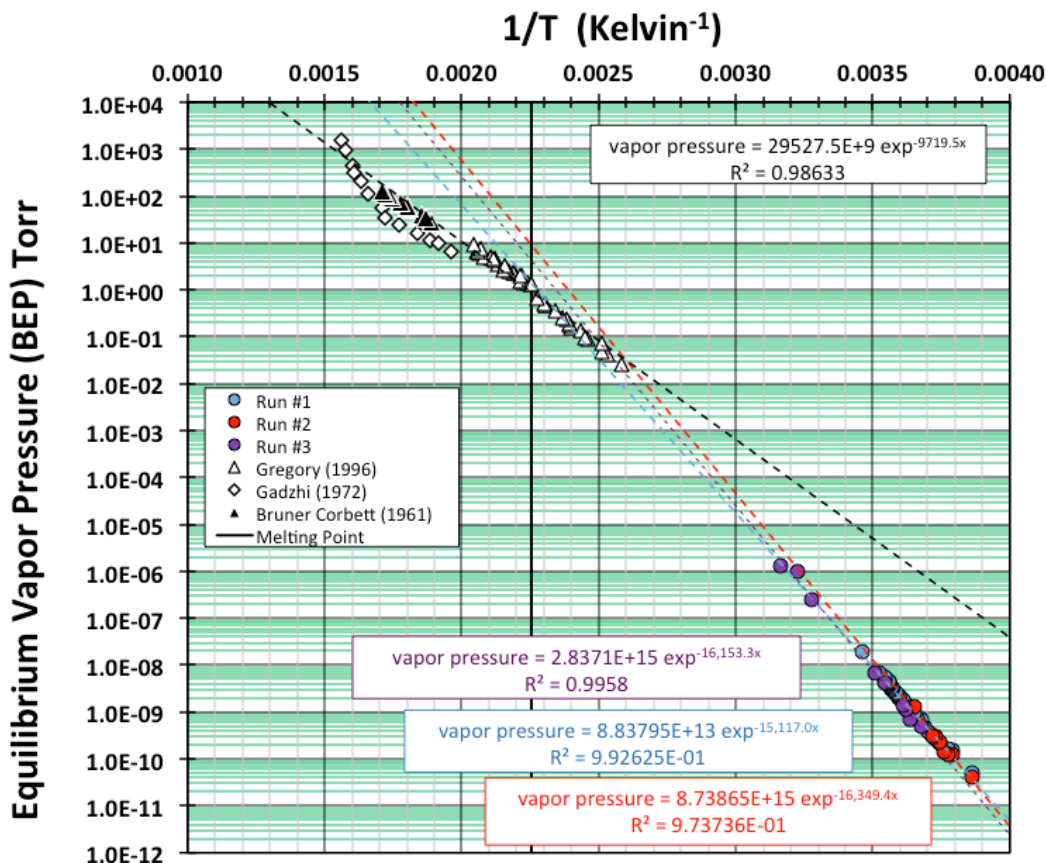


Fig. 2 Equilibrium vapor pressure of SbI_3 as a function of inverse temperature

For the analysis, the pressure was determined as the average of the 3 separate data collections ranging from below room temperature, $-14\text{ }^\circ\text{C}$, to slightly above room temperature, $43\text{ }^\circ\text{C}$. As shown in Fig. 2, the obtained data were self-consistent with little divergence. In this temperature range, the slope of the averaged pressure data from 3 collections is $(\Delta H_{\text{vapor}}/R)$ and follows the exponential of $(-15,452.91/T)$ and yields $\Delta H_{\text{vapor}} = -128.48\text{ kJ/mol}$.

Further, the extrapolation to higher-temperature data show reasonable consistency with previously published data; the data would connect to form a piecewise continuous curve. There is some nonlinearity and softening in the global slope as the melting point is approached, and then surpassed. On Fig. 2, the previously published data suggest a softer $(\Delta H_{\text{vapor}}/R)$ slope, which is found to be $(-9719.5/T)$, and that suggests a softening of the enthalpy of vaporization to

$\Delta H_{\text{vapor}} = 80.81$ kJ/mol. In the mid-temperature range, as the melting point is approached, the $(\Delta H_{\text{vapor}}/R)$ slope moderates to an intermediate value of $\Delta H_{\text{vapor}} = 87.6$ kJ/mol. This progressive reduction is most likely associated with increased translational, rotational, and vibrational entropies and larger-amplitude intermolecular oscillation as the solid approaches the melting point.

The melting point of SbI_3 is 170.6 °C and is indicated on Fig. 2 by the vertical black line intersecting the x-axis at approximately $1/T = 0.00225/\text{K}$. Above the melting point, there are more divergent data sets from previously published work that imply the thermal decomposition of SbI_3 into unknown subspecies, which are not relevant to the present work.

4. Discussion and Measurements

Bruner and Corbett⁵ published results from their study of the vapor pressure of SbI_3 at very high temperatures as a step toward understanding the high-temperature behavior of new linear-molecule structural forms of halide given by the reaction $4\text{SbI}_3 + 2\text{Sb} = 3\text{Sb}_2\text{I}_4$. For pure liquid SbI_3 , however, they reported a similar nonlinearity (softening) in the pressure data as temperature is increased, and at high temperature in the range of 260 °C and extending to 405 °C. They reported that their analysis of the pressure data for SbI_3 yielded $\Delta H_{\text{vapor}} = -64$ kJ/mol near the boiling point of 401.6 °C.

Gadzhi and coworkers⁶ measured the vapor pressure at a similar but hotter range than that investigated by Bruner and Corbett. Because their data include the highest temperatures ever recorded, there is likely some chemical decomposition of SbI_3 (cracking) into distinct species such as free I and $\text{SbI}_{(3-x)}$ with a concomitant supra nonlinear increase in the vapor pressure at the highest temperatures.

Ferro and colleagues⁷ studied vapor pressure as a step toward understanding vapor transport of chemical species. In contrast to the earlier work of Bruner and Corbett, Ferro and colleagues' work focused on colder SbI_3 solid near the melting point, and thus a much lower-temperature range: starting at 109 °C and extending to 277 °C. Using 2 different techniques to determine the equilibrium vapor pressure, they reported very linear behavior and $\Delta H_{\text{vapor}} = -109.3$ kJ/mol.

The work of Gregory⁸ did not focus on the determination of ΔH_{vapor} , but instead attempted to reconcile some of the apparent inconsistencies in vapor pressure across the entire temperature range of past work. Gregory used absorbance by the vapor phase as an index of vapor pressure. One finding Gregory validated was that the thermodynamic behavior of SbI_3 follows the trend of progressively reducing

ΔH_{vapor} as temperature increases. The measurements of Gregory were generally consistent with past work, and that suggests the nonlinear, softening ΔH_{vapor} with temperature of previous reports is generally consistent.

5. Significance

This work expands the breadth of vapor pressure measurement from the previous 6 orders of magnitude to 16 orders of magnitude, and represents a more comprehensive perspective of the equilibrium vapor pressure of this interesting and technologically important material. The present work is consistent with previous determinations of ΔH_{vapor} on the order of approximately 100 kJ/mol (Fig. 3). The broadly arcing curve suggests that the ΔH_{vapor} value one obtains is, in part, determined by the temperature where the data were measured: ΔH_{vapor} will be higher at lower temperature and lower at higher temperature. Ignoring entropy contributions to sublimation allows the contributions to the sublimation to be one lumped term called the effective enthalpy of sublimation. In that case, the effective ΔH_{vapor} of SbI_3 has a strong, nonlinear temperature dependence.

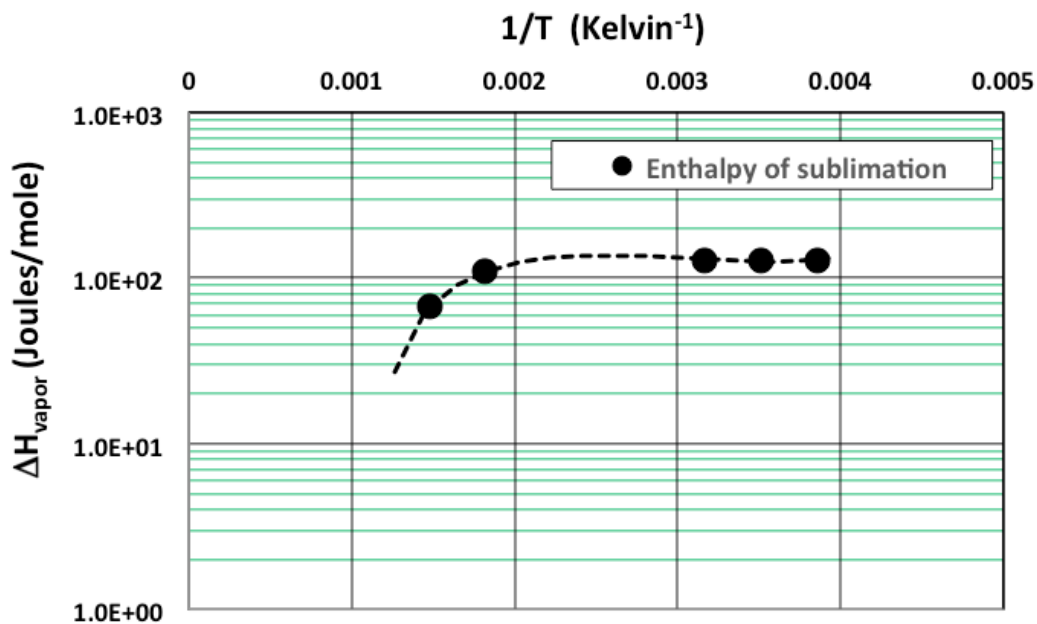


Fig. 3 Effective ΔH_{vapor} of SbI_3 as a function of temperature

6. MBE Doping Strategy

To be effective as a dopant, I must be incorporated within the $(\text{Bi,Sb})_2(\text{Te,Se})_3$ crystal lattice during growth. If one assumes unity incorporation (i.e., one I becomes incorporated from one SbI_3 molecule that hits the surface), then a simple ratio of pressures could yield an estimate of the obtained doping concentration. During $(\text{Bi,Sb})_2(\text{Te,Se})_3$ MBE growth, the growth rate is governed by the pressure of Bi metal. As a consequence of that, the ratio of SbI_3 pressure to Bi pressure can therefore be an approximate index for the expected doping concentration.

If, say, the overall concentration of desired doping for I atoms is approximately 5×10^{19} I atoms per cm^3 and assuming each I donates one extra electron, then that would yield an n-type carrier density of $5 \times 10^{19}/\text{cm}^3$. If the $(\text{Bi,Sb})_2(\text{Te,Se})_3$ matrix concentration is roughly 5×10^{23} atoms per cm^3 , then the preferred ratio of Bi pressure to SbI_3 pressure would be 10,000:1. For a common Bi pressure during $(\text{Bi,Sb})_2(\text{Te,Se})_3$ MBE growth, a Bi pressure of 5×10^{-7} Torr is not unreasonable. In the case where Bi pressure is 5×10^{-7} Torr, one would target an SbI_3 pressure of 5×10^{-11} Torr; refer to Fig. 2. One would, therefore, select an SbI_3 temperature of roughly -10 °C to achieve an SbI_3 pressure of 5×10^{-11} Torr, resulting in a doping concentration of $5 \times 10^{19}/\text{cm}^3$.

7. Conclusions

The equilibrium vapor pressure of SbI_3 has been measured over a temperature range from 253 to 320 K (-20 to 47 °C) using a classical Knudsen cell method. An analysis of the slope of that data as a function of temperature is one measure of the enthalpy of sublimation (ΔH_{vapor}), and a value of $\Delta H_{\text{vapor}} = -128.48$ kJ/mol has been obtained for SbI_3 .

8. References

1. Yim W, Fitzke E, Rosi F. Thermoelectric properties of $\text{Bi}_2\text{Te}_3\text{-Sb}_2\text{Te}_3\text{-Sb}_2\text{Se}_3$ pseudo-ternary alloys in the temperature range 77 to 300° K. *J Mat Sci.* 1966;1(1):52.
2. Taylor P, Maddux J, Jesser W, Rosi F. Room-temperature anisotropic, thermoelectric, and electrical properties of n-type $(\text{Bi}_2\text{Te}_3)_{90}(\text{Sb}_2\text{Te}_3)_5(\text{Sb}_2\text{Se}_3)_5$ and compensated p-type $(\text{Sb}_2\text{Te}_3)_{72}(\text{Bi}_2\text{Te}_3)_{25}(\text{Sb}_2\text{Se}_3)_3$ semiconductor alloys. *J Appl Physics.* 1999;85:7807.
3. Mzerd A, Sayah D, Tedenac JC, Boyer A. Optimal crystal growth conditions of thin films of BiTe semiconductors. *J Crystal Growth.* 1994;140(3):365.
4. Kuznetsov P, Yakushcheva G, Luzanov V, Temiryazev A, Shchamkhalova B, Jitov V, Sizov V. Metalorganic vapor phase epitaxy growth of ternary tetradymite BiTeSe compounds. *J Crystal Growth.* 2015;409:56.
5. Bruner B, Corbett J. A vapour-pressure study of the solution of antimony in liquid antimony (III) iodide—the formation of Sb_2I_4 . *J Inorganic and Nuclear Chem.* 1961;20(1-2):62.
6. Bakhyshev R, Gadzhiev C, Kuliev A. Thermodynamic properties of antimony triiodide. *Azerb Khim Zh.* 1972;1:103.
7. Ferro D, Nappi B, Piacente V. Vapour pressure of antimony triiodide. *J Chem Thermodynamics.* 1979;11:193.
8. Gregory N. Equilibrium vapor concentrations in the antimony + iodine system: molar absorptivities of antimony(III) iodide vapor. *J Chem Eng Data.* 1996;41:107.

List of Symbols, Abbreviations, and Acronyms

Bi	bismuth
I	iodine
MBE	molecular beam epitaxy
OMVPE	organometallic vapor phase epitaxy
P	pressure
p-BN	pyrolytic boron nitride
Sb	antimony
SbI ₃	antimony triiodide
Se	selenium
T	temperature
Te	tellurium
ΔH_{vapor}	enthalpy of vaporization
ΔV	net change in molar-specific volume

1 DEFENSE TECHNICAL
(PDF) INFORMATION CTR
DTIC OCA

2 DIR ARL
(PDF) IMAL HRA
RECORDS MGMT
RDRL DCL
TECH LIB

1 GOVT PRINTG OFC
(PDF) A MALHOTRA

3 DIR ARL
(PDF) RDRL SED E
PJ TAYLOR
C RONG
RDRL SEE I
R ENCK